

Stimulation of Sigma-1 Receptor Ameliorates Depressive-like Behaviors in CaMKIV Null Mice

Shigeki Moriguchi · Hiroyuki Sakagami · Yasushi Yabuki · Yuzuru Sasaki · Hisanao Izumi · Chen Zhang · Feng Han · Kohji Fukunaga

Received: 4 August 2014 / Accepted: 6 October 2014 / Published online: 15 October 2014
© Springer Science+Business Media New York 2014

Abstract Sigma-1 receptor (Sig-1R) is a molecular chaperone regulating calcium efflux from the neuronal endoplasmic reticulum to the mitochondria. Calcium/calmodulin-dependent protein kinase IV (CaMKIV) null mice exhibit depressive-like behaviors and impaired neurogenesis as assessed by bromodeoxyuridine (BrdU) incorporation into newborn cells of the hippocampal dentate gyrus (DG). Here, we demonstrate that chronic stimulation of Sig-1R by treatment with the agonist SA4503 or the SSRI fluvoxamine for 14 days improves depressive-like behaviors in CaMKIV null mice. By contrast, treatment with paroxetine, which lacks affinity for Sig-1R, did not alter these behaviors. Reduced numbers of BrdU-positive cells and decreased brain-derived neurotrophic factor (BDNF) mRNA expression and protein kinase B (Akt; Ser-473) phosphorylation seen in the DG of CaMKIV null mice were significantly rescued by chronic Sig-1R stimulation. Interestingly, reduced ATP production observed in the DG of CaMKIV null mice was improved by chronic Sig-1R stimulation. Such stimulation also improved hippocampal long-term potentiation (LTP) induction and maintenance, which are impaired in the DG of CaMKIV null mice. LTP rescue was closely associated with both increases

in calcium/calmodulin-dependent protein kinase II (CaMKII) autophosphorylation and GluA1 (Ser-831) phosphorylation. Taken together, Sig-1R stimulation by SA4503 or fluvoxamine treatment increased hippocampal neurogenesis, which is closely associated with amelioration of depressive-like behaviors in CaMKIV null mice.

Keywords Sigma-1R · CaMKIV null mice · Depressive-like behaviors · Hippocampal neurogenesis

Abbreviations

| | |
|--------|--|
| Akt | Protein kinase B |
| BDNF | Brain-derived neurotrophic factor |
| BrdU | Bromodeoxyuridine |
| CaMKII | Calcium/calmodulin-dependent protein kinase II |
| CaMKIV | Calcium/calmodulin-dependent protein kinase IV |
| CREB | cAMP-responsive element binding protein |
| DG | Dentate gyrus |
| DHEA | Dehydroepiandrosterone |
| ERK | Extracellular signal-regulated kinase |
| ER/SR | Endoplasmic/sarcoplasmic reticulum |
| fEPSPs | Field excitatory postsynaptic potentials |
| HFS | High-frequency stimulation |
| LTP | Long-term potentiation |
| NMDAR | N-methyl-D-aspartate receptor |
| Sig-1R | Sigma-1 receptor |
| SSRIs | Selective serotonin reuptake inhibitors |

S. Moriguchi (✉) · Y. Yabuki · Y. Sasaki · H. Izumi · K. Fukunaga (✉)
Department of Pharmacology, Graduate School of Pharmaceutical Sciences, Tohoku University, 6-3 Aramaki-Aoba, Aoba-ku, Sendai, Miyagi 980-8578, Japan
e-mail: shigeki@m.tohoku.ac.jp
e-mail: kfukunaga@m.tohoku.ac.jp

H. Sakagami
Department of Anatomy, Kitasato University School of Medicine, Sagami-hara, Japan

C. Zhang · F. Han
Department of Pharmacy, College of Pharmaceutical Sciences, Zhejiang University, Hangzhou, China

Introduction

Depressive-like behavior is believed to be associated with impaired adult neurogenesis in the subgranular zone of the hippocampal dentate gyrus (DG) [1]. Restricted exposure of the hippocampus to X-irradiation blocks DG neurogenesis

and compromises the ability of anti-depressants to improve depressive behaviors [2]. Human postmortem brain studies reveal that chronic treatment with tricyclic anti-depressants such as imipramine increases the number of neural progenitor cells in the DG in humans with major depression disorders [3]. Selective serotonin reuptake inhibitors (SSRIs) such as fluoxetine or fluvoxamine also improve impaired adult hippocampal neurogenesis in the rodent DG [2, 4]. Notably, SSRIs, including fluoxetine and fluvoxamine, and imipramine show an affinity for the sigma-1 receptor (Sig-1R) [5]. Knockout mice lacking Sig-1R exhibit depressive-like behaviors [6]. We also recently reported that impaired cognitive-related and depressive-like behaviors in olfactory bulbectomized mice are improved by chronic oral administration of dehydroepiandrosterone (DHEA), an endogenous Sig-1R ligand [7, 8].

Sig-1R has been cloned in humans and several species [9–13]. In the brain, Sig-1R is widely distributed in both neurons and in glial cells such as oligodendrocytes, and is especially enriched in the prefrontal cortex, hippocampus, and striatum [14, 15]. Sig-1R mainly localizes in membranes of the endoplasmic/sarcoplasmic reticulum (ER/SR) where it regulates Ca^{2+} signaling through the inositol 1,4,5-triphosphate receptor in ER membranes closely associated with mitochondria [16, 17]. Sig-1R stimulation increases release of the neurotransmitters dopamine and glutamate [18, 19]. However, the mechanism underlying this activity remains unclear.

Calcium/calmodulin-dependent protein kinase IV (CaMKIV) is a serine-threonine protein kinase activated by nuclear Ca^{2+} elevation and which mediates phosphorylation of cyclic AMP-responsive element binding protein (CREB) at residue Ser-133 [20, 21]. CREB phosphorylation by CaMKIV regulates expression of several genes (including *BDNF*) that function in synaptic plasticity [22], learning and memory [23–25], and emotional behaviors in rodents [26–28]. CaMKIV is widely distributed in the anterior cingulate cortex, somatosensory cortex, insular cortex, cerebellum, hippocampus, and amygdala, where the kinase is primarily localized to neuronal nuclei [29]. Accumulating evidence demonstrates that CaMKIV null mice display deficits in contextual and cued fear conditioning memory [30], decreased anxiety-like behaviors [30, 31], and impaired memory of eyeblink conditioning [32]. More importantly, treatment with the typical SSRI fluoxetine fails to induce DG neurogenesis and lacks of its anti-depressive activity in CaMKIV null mice [33].

Based on these findings, we concluded that CaMKIV null mice showing resistance to SSRI treatment constitute a useful model of refractory depression in which to test therapeutic strategies to improve these behaviors. Using novel therapeutics of SA4503 or fluvoxamine, we found that Sig-1R stimulation rescues impaired neurogenesis and improves depressive-like behaviors in these mice.

Materials and Methods

Generation of CaMKIV Null Mice CaMKIV null mice were established by Takao et al. [30]. To disrupt the CaMKIV gene, the exon containing the CaMKIV α initiation codon was replaced with a neomycin resistance cassette. Southern blot analysis with a 3' external probe confirmed homologous recombination in CCE embryonic stem (ES) cells derived from the 129/SvJ mouse strain. A more detailed protocol used to establish these mice is provided in our previous study [30]. Adult (8–9 weeks old) male CaMKIV null mice were housed in cages with free access to food and water at a constant temperature (23 ± 1 °C) and humidity (55 ± 5 %) with a 12-h light/dark cycle (09:00–21:00 hours). All experimental animal procedures were approved by the Committee on Animal Experiments at Tohoku University and Kitasato University.

Depressive-Like Behavioral Tasks (1) Tail suspension task: A detailed protocol of this task is described [8]. The test is based on the fact that normally, animals exhibit immobile posture when subjected to short-term, inescapable stress by tail suspension. (2) Forced swim task: The forced swim task is described elsewhere [8]. Mice are placed individually in glass cylinders (height, 20 cm; diameter, 15 cm) filled with 25 °C water and the duration of immobile periods within a 5-min test is scored.

Memory-Related Behavioral Tasks (1) Y-maze task: The Y-maze task is described elsewhere [7]. Spontaneous alternation behavior in a Y-maze is assessed as an indicator of spatial reference memory. The apparatus consists of three identical arms ($50\times 16\times 32$ cm) made of black Plexiglas. A mouse is placed at the end of one arm and allowed to move freely through the maze during an 8-min session to score the alteration behavior. (2) Novel object recognition task: A detailed protocol of this task has been reported [7]. The task is based on the tendency of normal rodents to discriminate a familiar from a new object. Mice are individually habituated to an open-field box ($35\times 25\times 35$ cm) for two consecutive days. The experimenter scoring behavior is blinded to the treatment. During the acquisition phases, two objects of the same material are placed in a symmetric position in the center of the chamber for 5 min. One hour later, one object is replaced by a novel object, and exploratory behavior is again analyzed for 5 min to score the number of approaching to two objects. (3) Step-through passive avoidance task: This task is described elsewhere [7]. Briefly, training and retention trials are conducted in box that consists of dark ($25\times 25\times 25$ cm) and light ($14\times 10\times 25$ cm) compartments. The floor is constructed of stainless steel rods; those in the dark compartment are connected to an electronic stimulator (Nihon Kohden, Tokyo, Japan). Mice are habituated to the apparatus the day before avoidance acquisition. On training trials, a mouse is placed in

the lighted compartment of the box. When the mouse enters the dark compartment, the door is closed and the animal receives an inescapable electric shock (1 mA for 500 ms) from the floor. The mouse is removed from the apparatus 30 s later. The same procedure without footshock is repeated 24 h later to assess retention level.

Electrophysiology Hippocampal slices were prepared as described [34]. Transverse hippocampal slices (400 μm thick) cut using a vibratome (Microslicer DTK-1000) were incubated for 2-h in continuously oxygenized (95 % O_2 , 5 % CO_2) artificial cerebrospinal fluid at room temperature. Then, slices were transferred to an interface recording chamber and perfused at a flow rate of 2 ml/min with artificial cerebrospinal fluid warmed to 34 $^\circ\text{C}$. Field excitatory postsynaptic potentials were evoked by a 0.05-Hz test stimulus through a bipolar stimulating electrode placed on the perforant path from the entorhinal cortex and recorded from the inside granule cell layer using a glass electrode filled with 3 M NaCl. High-frequency stimulation (HFS) of 100 Hz with a 1-s duration was applied twice with a 10-s interval, and test stimulation was continued for the indicated periods. After recording, slices were transferred to a plastic plate cooled on ice to dissect out the DG, which was immediately frozen in liquid nitrogen and stored at -80 $^\circ\text{C}$ until biochemical analysis was performed.

Biochemical Analysis Analysis was performed as described [34] using the following antibodies: anti-phospho CaMKII (1:5000 [35]), anti-CaMKII (1:5000 [36]), anti-phospho-GluA1 (Ser-831) (1:1000, Millipore, Billerica, MA, USA), anti-GluA1 (1:1000, Millipore), anti-phospho-Akt (Ser-473) (1:1000, Millipore), anti-Akt (1:1000, Millipore), anti-phospho-MAP kinase (diphosphorylated extracellular signal-regulated kinase (ERK) 1/2) (1:2000, Sigma-Aldrich, St. Louis, MO, USA), anti-MAP kinase (1:1000, Millipore), anti-CREB (Ser-133) (1:1000, Millipore), anti-CREB (1:1000, Millipore), anti-sigma-1R (1:1000, Abcam, Cambridge, MA, USA), and anti- β -tubulin (1:5000, Sigma-Aldrich). Bound antibodies were visualized using the enhanced chemiluminescence detection system (Amersham Life Science, Buckinghamshire, UK) and analyzed semiquantitatively using the National Institutes of Health Image program.

Immunohistochemistry Immunohistochemistry was performed as described [8, 30]. Mice at 10–12 weeks of age were anesthetized with sevoflurane and perfused via the ascending aorta with phosphate-buffered saline (PBS; pH 7.4) until the outflow became clear. The perfusate was then switched to phosphate buffer (pH 7.4) containing 4 % paraformaldehyde in 0.1 M phosphate buffer (pH 7.4) for 15 min. The brain was removed, postfixed in the same solution for 2 h at 4 $^\circ\text{C}$, embedded in 2 % agarose and sliced at 50 μm using a

vibratome (Dosaka EM Co. Ltd., Kyoto, Japan, or Leica VT1000S, Nussloch, Germany). Coronal brain sections were permeabilized with 0.3 % Triton X-100 in PBS and blocked with 5 % normal goat or donkey serum for 3 h and then incubated overnight with mouse anti-NeuN monoclonal antibody (1:500) (Millipore), anti-Sigma-1R polyclonal antibody (1:500) (Abcam), a rat anti-bromodeoxyuridine (BrdU) polyclonal antibody (1:500) (Accurate Chemical and Scientific, Oxford Biotechnology, Oxfordshire, UK), anti-PSD95 monoclonal antibody (1:500) (Abcam), anti-Synaptophysin monoclonal antibody (1:500) (Sigma-Aldrich), anti-CaMKIV polyclonal antibody (1:500 [30]), anti-BLBP monoclonal antibody (1:500, BLBP-GF-Af291, Frontier Institute Co., Ltd., Hokkaido, Japan), anti-PSA-NCAM monoclonal antibody (1:500 [37]), or anti-calbindin polyclonal antibody (1:500, Santa Cruz Biotech, Santa Cruz, CA) in blocking solution at 4 $^\circ\text{C}$. After thorough washing in PBS, sections were incubated 3-h in Alexa 488-labeled anti-rat IgG (anti-BrdU) or Alexa 594-labeled anti-mouse IgG (anti-NeuN). After several PBS washes, sections were mounted on slides with Vectashield (Vector Laboratories, Burlingame, CA, USA). Immunofluorescent images were analyzed using a confocal laser-scanning microscope (Nikon EZ-C1, Nikon, Tokyo, Japan or LSM 710, Zeiss, Oberkochen, Germany). To count BrdU and NeuN double-positive cells after immunohistochemistry, six hippocampal sections were cut every 50 μm beginning at 1.7 to 2.2 mm caudal to the bregma. The number of BrdU/NeuN or BrdU/ β -catenin double-positive cells in the DG region was determined in a 300×300 - μm area in a section. In the DG, the GCL (approximately 50 μm wide) and the SGZ (defined as a zone two cell bodies wide (5 μm) along the border of the GCL and hilus) were quantified together. The number of BrdU/NeuN double-positive cells counted per mouse was expressed as the number of the double-positive cells per a 300×300 - μm area. Six sections per mouse and six mice per condition were used. The person responsible for cell counts was blind to experimental conditions.

ATP Assay DG samples were dissected, rapidly frozen in liquid nitrogen and stored at -80 $^\circ\text{C}$ before use. ATP measurement was performed using an ATP assay kit (Toyo Ink, Tokyo, Japan), according to the manufacturer's protocol. Briefly, frozen samples were homogenized in homogenate buffer (0.25 M sucrose, 10 mM HEPES-NaOH, pH 7.4), and lysates were cleared by centrifugation at 1000g for 10 min at 4 $^\circ\text{C}$. The supernatant was collected, and supernatant proteins were solubilized in extraction buffer. After 30 min, buffer containing luciferin was added to each sample and oxyluciferin was detected using a luminometer (Gene Light 55, Microtec, Funabashi, Japan).

Real-Time PCR Quantification of BDNF mRNA Analysis was performed in 48-well plates (Mini Opticon Real Time PCR

System, Bio-Rad) using iQ SYBR Green Supermix 2× (Bio-Rad). Primer sequences used were: BDNF-IF (CCTGCATC TGTTGGGAGAC), BDNF-IR (GCCTTGTCCTGGACGTTTA), BDNF-IVF (CAGAGCAGCTGCCTTGATGT), BDNF-IVR (GCCTTGTCCTGGACGTTTA), GAPDH-F (TGTGTCCGTCGTGGATCTGA), and GAPDH-R (CACCACCTTCTTGATGTCATCATA). Relative quantities of target transcripts were determined by the comparative threshold cycle (Δ CT) method and normalized to GAPDH. Product purity and specificity were confirmed by omitting the template and performing a standard melting curve analysis.

Other Chemicals Paroxetine, fluvoxamine, DL-2-amino-5-phosphonovaleric acid (APV), nifedipine, and BrdU were purchased from Sigma-Aldrich (Tokyo, Japan). NE-100 was purchased from Santa Cruz Biotechnology, Inc. (Santa Cruz, CA, USA). SA4503 was synthesized in the Laboratory of Medical Chemistry, Zhejiang University (Hangzhou, China).

Data Analysis Comparison between two experimental groups was made using the unpaired Student's *t* test. Statistical significance for differences among groups was tested by one-way analysis of variance (ANOVA), followed by multiple comparisons between control and other groups using Scheffe's test by StatView (Hulinks, Inc). $P < 0.05$ was considered significant.

Results

Fluvoxamine or SA4503 Treatment Ameliorates Depressive-like Behaviors in CaMKIV Null Mice

To determine whether Sig-1R stimulation improves depressive-like behaviors in CaMKIV null mice, we tested the effects of the SSRI fluvoxamine, which has a high affinity for Sig-1R, the Sig-1R agonist SA4503, and paroxetine, an SSRI that lacks Sig-1R affinity, in these mice. Mice were treated chronically with paroxetine at 1.0 mg/kg, p.o., fluvoxamine at 2.5 mg/kg, p.o., or SA4503 at 0.3 mg/kg, p.o. for 14 days and then subjected to a tail suspension task. Immobility time was significantly increased in CaMKIV null compared to wild-type mice (wild-type mice, 127.8 ± 5.1 s, $n = 5$; CaMKIV null mice, 172.8 ± 7.9 s, $n = 5$), indicative of depressive-like behavior in the null group. Interestingly, chronic treatment with fluvoxamine or SA4503, but not with paroxetine, significantly decreased immobility time (fluvoxamine-treated CaMKIV null mice, 130.4 ± 7.3 s, $n = 5$; SA4503-treated CaMKIV null mice, 122.4 ± 8.8 s, $n = 5$) (Fig. 1a). Pretreatment of CaMKIV null mice with the Sig-

1R antagonist NE100 (1 mg/kg, i.p.) eliminated the effects of either fluvoxamine or SA4503 in CaMKIV null mice (NE100 plus fluvoxamine-treated CaMKIV null mice, 165.1 ± 11.1 s, $n = 5$; NE100 plus SA4503-treated CaMKIV null mice, 162.3 ± 9.9 s, $n = 5$) (Fig. 1a).

CaMKIV null mice also showed significantly increased immobility time relative to wild-type mice in a forced swimming task (wild-type mice, 44.7 ± 2.5 s, $n = 5$; CaMKIV null mice, 86.7 ± 8.5 s, $n = 5$). Chronic fluvoxamine or SA4503 treatment, but not treatment with paroxetine, significantly ameliorated decreased immobility time (fluvoxamine-treated CaMKIV null mice, 62.0 ± 4.9 s, $n = 5$; SA4503-treated CaMKIV null mice, 64.8 ± 4.6 s, $n = 5$) (Fig. 1b). Pretreatment with NE100 (1.0 mg/kg, i.p.) significantly canceled the effects of fluvoxamine or SA4503 treatments in CaMKIV null mice (NE100 plus fluvoxamine-treated CaMKIV null mice, 92.5 ± 10.2 s, $n = 5$; NE100 plus SA4503-treated CaMKIV null mice, 96.1 ± 7.3 s, $n = 5$) (Fig. 1b).

Notably, CaMKIV null mice showed normal memory-related behaviors, as assessed by Y-maze ($n = 6$) (Fig. 1c, d), novel object recognition ($n = 6$) (Fig. 1e) or passive avoidance tasks ($n = 6$) (Fig. 1f, g).

Fluvoxamine or SA4503 Treatment Ameliorates Decreased Hippocampal Neurogenesis in CaMKIV Null Mice

To address mechanisms underlying anti-depressive effects of fluvoxamine and SA4503, we evaluated hippocampal neurogenesis in CaMKIV null mice. Mice were injected with BrdU on the first day of drug treatment for five consecutive days during 2 weeks treatment with drugs. To identify BrdU-positive neuronal cells, hippocampal slices were double-stained with antibodies to BrdU and the neuronal marker NeuN. As compared to wild-type mice (Fig. 2a), the number of BrdU-positive neuronal cells significantly decreased in CaMKIV null mice (wild-type mice, 104.8 ± 2.4 cells, $n = 8$; CaMKIV null mice, 71.8 ± 3.1 cells, $n = 8$) (Fig. 2a, b). Chronic treatment with fluvoxamine (2.5 mg/kg) or SA4503 (0.3 mg/kg), but not paroxetine at 1.0 mg/kg, for 14 days significantly increased the number of BrdU/NeuN double-positive cells in CaMKIV null relative to wild-type mice (fluvoxamine-treated CaMKIV null mice, 111.1 ± 2.5 cells, $n = 8$; SA4503-treated CaMKIV null mice, 92.4 ± 2.3 cells, $n = 8$) (Fig. 2a, b). Pretreatment of CaMKIV null mice with NE100 (1.0 mg/kg i.p.) eliminated the effects of fluvoxamine or SA4503 in CaMKIV null mice (NE100 plus fluvoxamine-treated CaMKIV null mice, 66.2 ± 3.8 cells, $n = 8$; NE100 plus SA4503-treated CaMKIV null mice, 59.8 ± 6.3 cells, $n = 8$) (Fig. 2a, b).

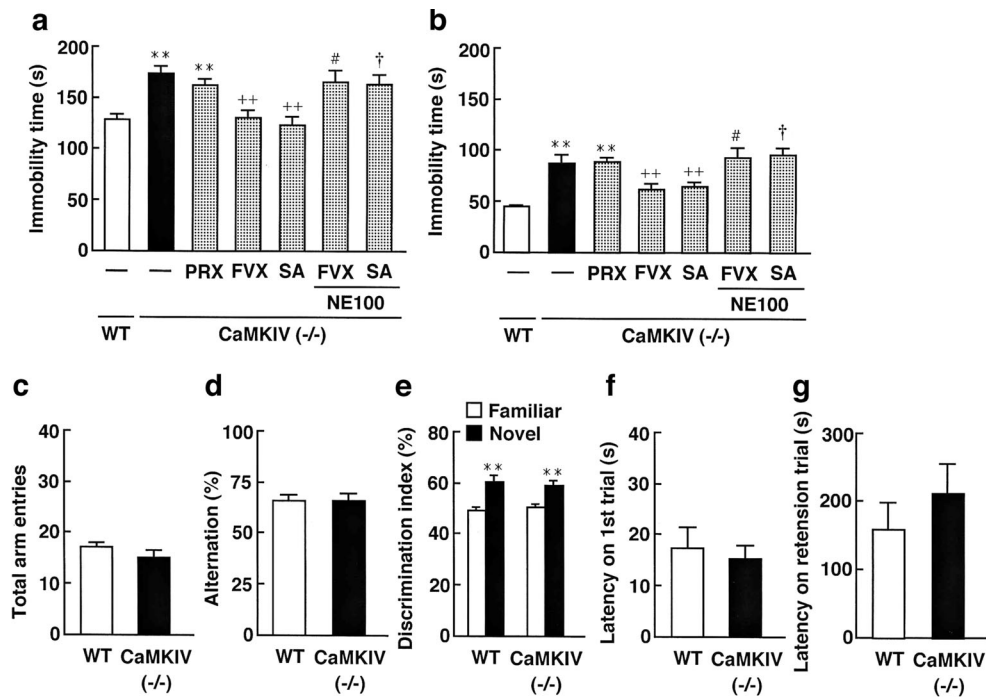


Fig. 1 Fluvoxamine or SA4503 but not paroxetine improves depressive-like behaviors in CaMKIV null mice. **a–b** Immobility time as determined by tail suspension task (**a**) or forced swim task (**b**) were measured following chronic treatment with paroxetine at 1.0 mg/kg, p.o., fluvoxamine at 2.5 mg/kg, p.o., or SA4503 at 0.3 mg/kg, p.o. for 14 days. Fluvoxamine or SA4503 significantly rescued increased immobility time seen in CaMKIV null mice, an effect blocked by pretreatment of NE100 at 1.0 mg/kg, i.p. (Mann-Whitney *U* test, $n=5$ per group). **c–d** Locomotor activity as assessed by total arm entries and alternation in a Y-maze task were measured in CaMKIV null and wild-type (WT) mice. No

differences in either were seen in CaMKIV null versus wild-type mice. **e** Shown are results from a novel object recognition task. There were no differences in discrimination of a novel object seen between CaMKIV null and wild-type mice. **f–g** Shown is latency time in a passive avoidance task. CaMKIV null and wild-type mice showed no significant differences. Vertical lines show the S.E.M. ** $p<0.01$ versus the wild-type mice. ++ $p<0.01$ versus CaMKIV null mice. # $p<0.05$ versus fluvoxamine-treated CaMKIV null mice. † $p<0.05$ versus SA4503-treated CaMKIV null mice

Fluvoxamine or SA4503 Treatment Improves Decreased CREB and Akt Phosphorylation, CaMKII α Autophosphorylation and BDNF Expression in the DG of CaMKIV Null Mice

Since activities of the phosphatidylinositol 3-kinase (PI3K)/Akt pathway and ERK signaling are required for proliferation and maturation of neural progenitor cells [38], we assessed those activities following fluvoxamine or SA4503-induced hippocampal neurogenesis in the DG of CaMKIV null mice. In those mice, phosphorylation of Akt (Ser-473) and CREB (Ser-133) in the DG was markedly decreased compared to wild-type mice (Akt (Ser-473), 60.0 \pm 7.2 % of control, $n=4$; CREB (Ser-133), 31.5 \pm 4.9 % of control, $n=4$) (Fig. 3a, b). Chronic treatment with fluvoxamine (2.5 mg/kg) or SA4503 (0.3 mg/kg), but not with paroxetine (1.0 mg/kg), significantly restored phosphorylation of Akt (Ser-473) and CREB (Ser-133) in the DG (fluvoxamine-treated CaMKIV null mice: Akt (Ser-473), 86.7 \pm 7.9 % of control, $n=4$; CREB (Ser-133), 52.9 \pm 2.6 % of control, $n=4$; SA4503-treated CaMKIV null mice: Akt (Ser-473), 95.0 \pm 9.1 % of control, $n=4$; CREB (Ser-133): 61.4 \pm 1.7 % of control, $n=4$) (Fig. 3a, b). Pretreatment with NE100 (1.0 mg/kg) completely eliminated

increased phosphorylation of Akt (Ser-473) and CREB (Ser-133) in the DG (NE100 plus fluvoxamine-treated CaMKIV null mice: Akt (Ser-473), 51.2 \pm 2.8 % of control, $n=4$; CREB (Ser-133), 32.1 \pm 6.0 % of control, $n=4$; NE100 plus SA4503-treated CaMKIV null mice: Akt (Ser-473), 48.6 \pm 3.4 % of control, $n=4$; CREB (Ser-133), 31.8 \pm 6.4 % of control, $n=4$) (Fig. 3a, b).

By contrast, phosphorylation of ERK (Thr-202/Tyr-204) in the DG of CaMKIV null mice was unchanged compared to wild-type mice. However, SA4503 treatment (0.3 mg/kg) significantly increased ERK phosphorylation (ERK, 160.4 \pm 9.3 % of control, $n=4$) and increased ERK phosphorylation was inhibited by NE100 (1.0 mg/kg) treatment (ERK, 94.9 \pm 3.1 % of control, $n=4$) (Fig. 3c, d). Interestingly, CaMKII α (Thr-286) autophosphorylation and GluA1 (Ser-831) phosphorylation were significantly decreased in the DG of CaMKIV null mice (CaMKII α (Thr-286), 57.4 \pm 3.5 % of control, $n=4$; GluA1 (Ser-831), 54.86 \pm 2.5 % of control, $n=4$) (Fig. 3c, d). Chronic treatment with fluvoxamine (2.5 mg/kg) or SA4503 (0.3 mg/kg), but not paroxetine (1.0 mg/kg), significantly rescued decreased CaMKII α (Thr-286) autophosphorylation and GluA1 (Ser-831) phosphorylation (fluvoxamine-treated CaMKIV null

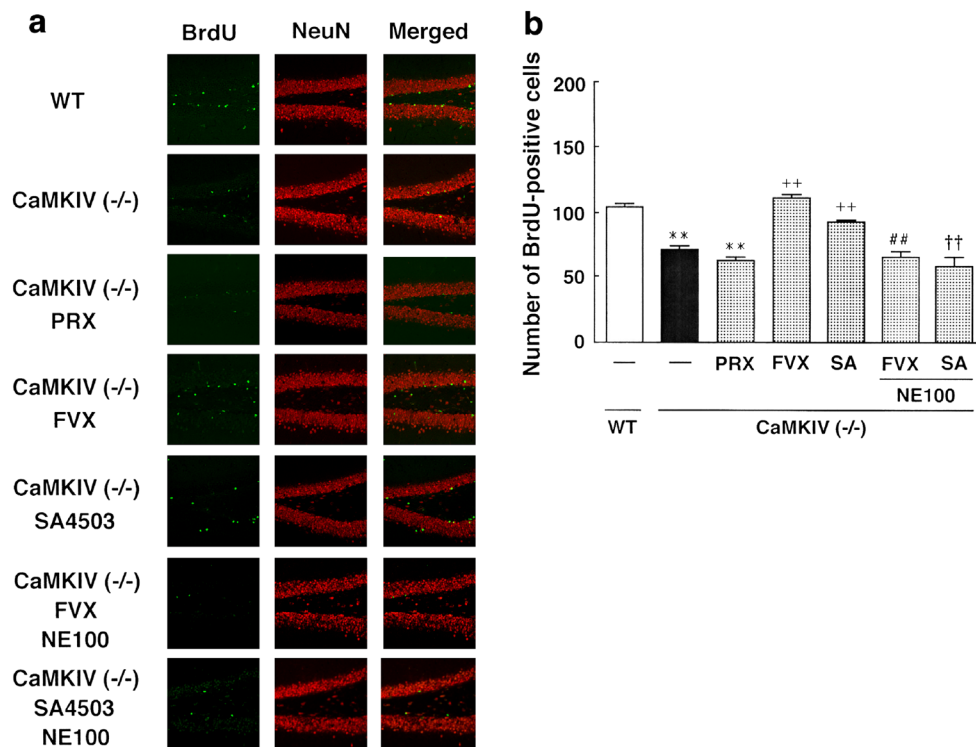


Fig. 2 Fluvoxamine or SA4503 but not paroxetine enhances hippocampal neurogenesis in CaMKIV null mice. **a** Confocal microscopy images showing double staining for BrdU (green), NeuN (red) and merged images in hippocampal slices from wild-type mice, CaMKIV null mice, paroxetine-treated CaMKIV null mice, fluvoxamine-treated CaMKIV null mice, SA4503-treated CaMKIV null mice, NE100 plus fluvoxamine-treated CaMKIV null mice and NE100 plus SA4503-treated CaMKIV null mice. Mice were injected with BrdU on the first day of

drug treatment for consecutive 5 days during 2 weeks treatment with drugs. Mice were treated with paroxetine, fluvoxamine, or SA4503 treatments for 2 weeks ($n=8$). **b** Quantitative analyses of the number of BrdU/NeuN double-positive cells in the DG ($n=8$). Vertical lines show SEM. ** $p<0.01$ versus wild-type mice. ++ $p<0.01$ versus CaMKIV null mice. ## $p<0.01$ versus fluvoxamine-treated CaMKIV null mice. †† $p<0.01$ versus SA4503-treated CaMKIV null mice

mice: CaMKII α (Thr-286), 93.0 ± 6.9 % of control, $n=4$; GluA1 (Ser-831), 90.7 ± 9.7 % of control, $n=4$; SA4503-treated CaMKIV null mice, CaMKII α (Thr-286), 93.9 ± 8.6 % of control, $n=4$; GluA1 (Ser-831), 99.3 ± 4.8 % of control, $n=4$) (Fig. 3c, d). Pretreatment with NE100 (1.0 mg/kg) eliminated CaMKII α (Thr-286) autophosphorylation and GluA1 (Ser-831) phosphorylation increased by fluvoxamine or SA4503 treatment (NE100 plus fluvoxamine-treated CaMKIV null mice: CaMKII α (Thr-286), 52.5 ± 1.7 % of control, $n=4$; GluA1 (Ser-831), 57.7 ± 4.2 % of control, $n=4$; NE100 plus SA4503-treated CaMKIV null mice: CaMKII α (Thr-286), 50.8 ± 2.5 % of control, $n=4$; GluA1 (Ser-831), 54.1 ± 3.1 % of control, $n=4$) (Fig. 3c, d).

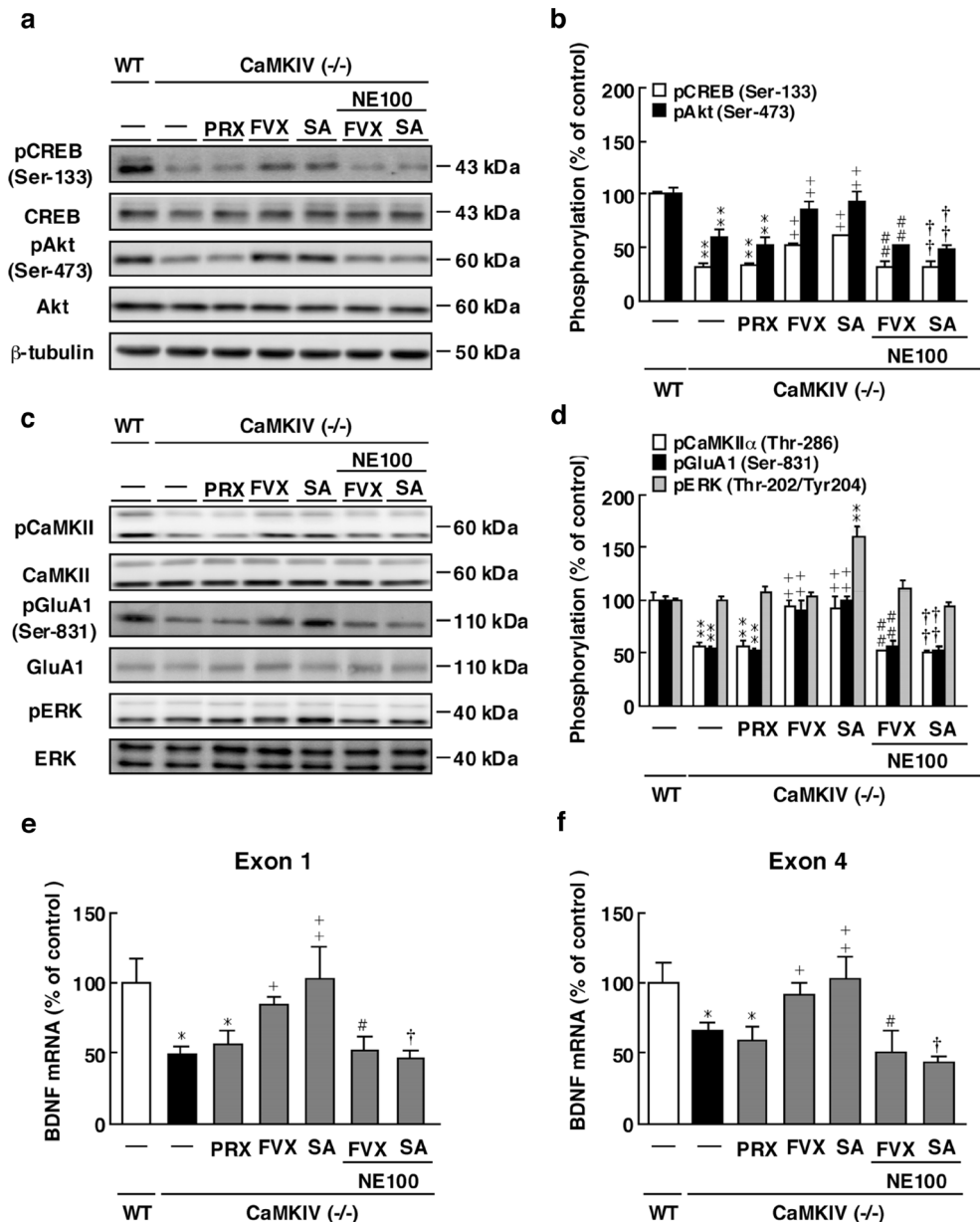
We next examined levels of transcripts encoding brain-derived neurotrophic factor (BDNF) in the DG. Since BDNF exons I and IV required Ca²⁺ signal [39, 40], we assessed levels of BDNF transcripts containing exons I and IV. In CaMKIV null versus wild-type mice, expression levels of BDNF mRNA containing those exons significantly decreased in the DG (Exon I, 49.1 ± 5.5 % of control, $n=10$; Exon IV, 65.5 ± 5.6 % of control, $n=10$). Chronic treatment with fluvoxamine or SA4503, but not with paroxetine, restored

levels of transcripts containing both exons in the DG (fluvoxamine-treated CaMKIV null mice: Exon I, 83.7 ± 6.1 % of control, $n=10$; Exon IV, 101.6 ± 22.4 % of control, $n=10$; SA4503-treated CaMKIV null mice: Exon I, 91.9 ± 7.3 % of control, $n=10$; Exon IV, 101.6 ± 22.4 % of control, $n=10$) (Fig. 3e, f). Pretreatment with NE100 (1.0 mg/kg) completely eliminated these effects (NE100 plus fluvoxamine-treated CaMKIV null mice: Exon I, 51.0 ± 13.8 % of control, $n=10$; Exon IV, 46.4 ± 5.3 % of control, $n=10$; NE100 plus SA4503-treated CaMKIV null mice: Exon I, 50.4 ± 23.8 % of control, $n=10$; Exon IV, 43.2 ± 5.0 % of control, $n=10$) (Fig. 3e, f).

Fluvoxamine or SA4503 Treatment Restores Decreased Expression of Sig-1R and ATP Production in the DG of CaMKIV Null Mice

Since we hypothesized that fluvoxamine and SA4503 elicit anti-depressive effects through Sig-1R stimulation, as reported previously [8], we next assessed localization of Sig-1R protein in the wild-type hippocampus. Hippocampal slices were double-stained with antibodies against Sig-1R and PSD95 or synaptophysin as postsynaptic or presynaptic

Fig. 3 Fluvoxamine or SA4503 treatment but not paroxetine rescues decreased phosphorylation of CREB (Ser-133), Akt (Ser-473) and CaMKII α (Thr-286) autophosphorylation and reduced BDNF mRNA expression in the DG of CaMKIV null mice. **a** or **c** Representative images of immunoblots using antibodies against phosphorylated CREB (Ser-133), CREB, phosphorylated Akt (Ser-473), Akt, autophosphorylated CaMKII, CaMKII, phosphorylated GluA1 (Ser-831), GluA1, phosphorylated ERK (Thr-202/Tyr-204), ERK and β -tubulin. **b** or **d** Quantitative analyses of phosphorylated CREB (Ser-133), phosphorylated Akt (Ser-473), autophosphorylated CaMKII α (Thr-286), phosphorylated GluA1 (Ser-831) and phosphorylated ERK (Thr-202/Tyr-204). **e–f** Quantitative analyses of BDNF mRNA containing exon I (**e**) or exon IV (**f**). Vertical lines show SEM. * p <0.05, ** p <0.01 versus wild-type mice. ^+p <0.05, ^{++}p <0.01 versus CaMKIV null mice. # p <0.05, $^{##}p$ <0.01 versus fluvoxamine-treated CaMKIV null mice. $^{\dagger}p$ <0.05, $^{\dagger\dagger}p$ <0.01 versus SA4503-treated CaMKIV null mice



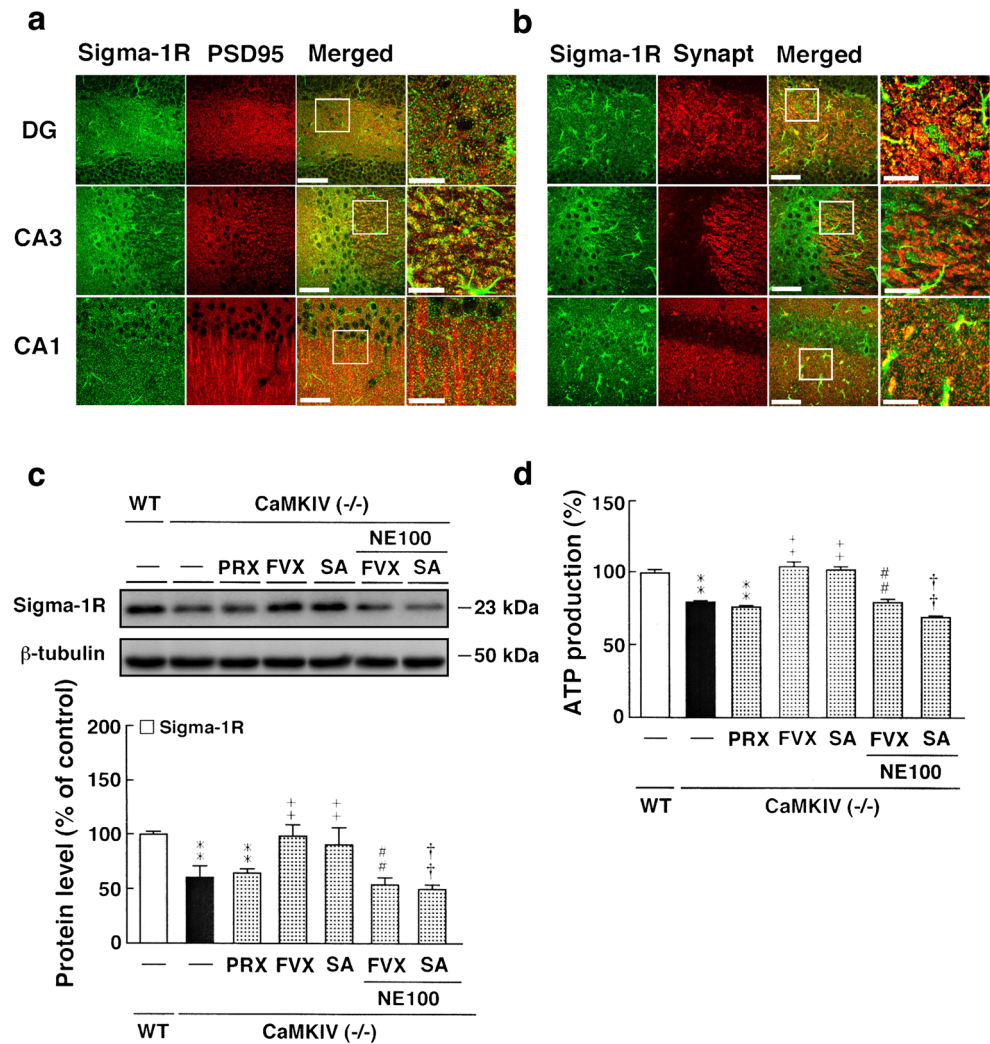
markers, respectively. Although Sig-1R was reported to be highly expressed in astrocytes [41], Sig-1R was moderately expressed in cell bodies of pyramidal neurons in hippocampal regions CA3 and CA1 and faintly in DG granule cells. In all of these regions, Sig-1R colocalized with PSD95 immunoreactivity in postsynaptic regions and was expressed in some presynaptic terminal co-expressing synaptophysin in the DG (Fig. 4a, b).

We next assessed Sig-1R protein levels in wild-type and CaMKIV null mice by immunoblot. Sig-1R levels significantly decreased in the DG of CaMKIV null mice (61.5 ± 10.1 % of control, $n=4$). Chronic treatment with fluvoxamine or SA4503, but not with paroxetine, significantly rescued decreased Sig-1R expression in the DG (fluvoxamine-treated

CaMKIV null mice, 99.9 ± 9.7 % of control, $n=4$; SA4503-treated CaMKIV null mice, 91.8 ± 15.4 % of control, $n=4$). Enhancement of Sig-1R expression by fluvoxamine or SA4503 was eliminated by NE100 treatment (1.0 mg/kg) (NE100 plus fluvoxamine-treated CaMKIV null mice, 53.9 ± 6.9 % of control, $n=4$; NE100 plus SA4503-treated CaMKIV null mice, 50.9 ± 3.9 % of control, $n=4$) (Fig. 4c).

We previously reported that Sig-1R stimulation elicits mitochondria-dependent ATP production [17]. Therefore, we assessed ATP content in the DG of CaMKIV null mice. ATP production significantly decreased in the DG of CaMKIV null relative to wild-type mice, similar to Sig-1R expression levels (80.3 ± 1.2 % of control, $n=4$). Chronic treatment with fluvoxamine or SA4503, but not with paroxetine, significantly

Fig. 4 Fluvoxamine or SA4503 treatment but not paroxetine restores decrease in Sig-1R and ATP production in the DG of CaMKIV null mice. **a–b** Confocal microscopy images showing double staining for Sig-1R (green), PSD95 (a) or synaptophysin (b) (red) and merged images in hippocampal slices. *Far right columns* show high magnification images of boxed regions in adjacent image. *Scale bars*, a and b, 50 μ m in low magnification and 20 μ m in high magnification images. **c** Representative images of immunoblots using antibodies against Sig-1R and quantitative analyses of ATP production. *Vertical lines* show SEM. ****** $p < 0.01$ versus wild-type mice. **++** $p < 0.01$ versus CaMKIV null mice. **##** $p < 0.01$ versus fluvoxamine-treated CaMKIV null mice. **††** $p < 0.01$ versus SA4503-treated CaMKIV null mice



restored decreased ATP production in the DG of CaMKIV null mice (fluvoxamine-treated CaMKIV null mice, 104.7 ± 3.3 % of control, $n=4$; SA4503-treated CaMKIV null mice, 102.7 ± 2.6 % of control, $n=4$) (Fig. 4d), and ATP production enhanced by fluvoxamine or SA4503 was inhibited by NE100 (1.0 mg/kg) (NE100 plus fluvoxamine-treated CaMKIV null mice, 79.6 ± 3.2 % of control, $n=4$; NE100 plus SA4503-treated CaMKIV null mice, 69.7 ± 1.1 % of control, $n=4$) (Fig. 4d).

SA4503 Treatment Rescues Decreased Long-Term Potentiation in the DG of CaMKIV Null Mice

We previously reported that stimulation of Sig-1R by chronic DHEA treatment ameliorates impaired long-term potentiation (LTP) in the hippocampal DG of OBX mice [8]. Therefore, we analyzed LTP in the DG of wild-type mice, CaMKIV null mice, and CaMKIV null mice treated every day for 14 days with SA4503. In control slices from wild-type mice, HFS (100 Hz, 2 trains) of the inside granule cell layer induced

LTP in the DG, which lasted over 60 min (146.3 ± 6.2 % of baseline at 60 min, $n=5$) (Fig. 5a–c). However, relative to wild-type mice, markedly reduced LTP was observed in the DG of CaMKIV null mice (122.0 ± 5.8 % of baseline at 60 min, $n=5$) (Fig. 5a–c). SA4503 treatment significantly improved LTP in the DG of CaMKIV null mice (150.2 ± 8.4 % of baseline at 60 min, $n=5$) (Fig. 5a–c). Enhancement of LTP by SA4503 was eliminated by NE100 treatment (1.0 mg/kg) (121.2 ± 7.1 % of baseline at 60 min, $n=4$) (Fig. 5a–c).

Elevation of CaMKII α Autophosphorylation by SA4503 Treatment is Inhibited by APV in the DG of CaMKIV Null Mice

We also examined that mechanism of elevation of CaMKII activity by Sig-1R stimulation in the DG of CaMKIV null mice. In hippocampal DG slices of CaMKIV null mice, acute treatment with SA4503 (1 μ M) significantly restored down-regulated CaMKII α (Thr-286) autophosphorylation relative

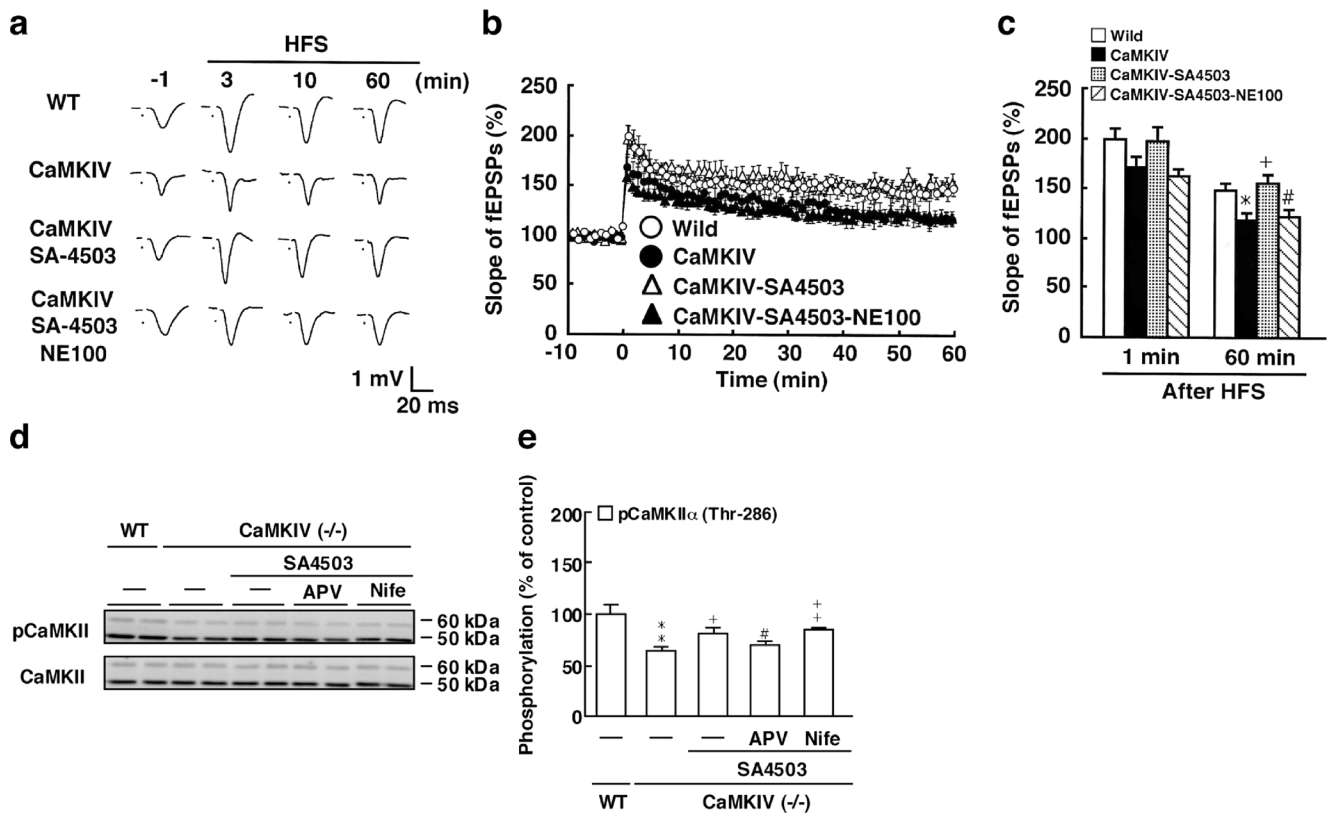


Fig. 5 SA4503 ameliorates impaired LTP seen in the DG of CaMKIV null mice. **a** Representative field excitatory postsynaptic potentials (fEPSPs) were recorded from the DG of wild-type mice, CaMKIV null mice, SA4503-treated CaMKIV null mice, and SA4503 plus NE100-treated CaMKIV null mice. SA4503 treatment significantly improved impaired LTP in CaMKIV null mice. **b–c** Changes in fEPSP slope following HFS are shown in wild-type mice, CaMKIV null mice, SA4503-

treated CaMKIV null mice, and SA4503 plus NE100-treated CaMKIV null mice. **d** Representative images of immunoblots using antibodies against autophosphorylated CaMKII and CaMKII. **e** Quantitative analyses of autophosphorylated CaMKII α (Thr-286). Vertical lines show SEM. * $p < 0.05$; ** $p < 0.01$ versus wild-type mice. + $p < 0.05$; ++ $p < 0.01$ versus CaMKIV null mice. # $p < 0.05$ versus SA4503-treated CaMKIV null mice

to wild-type mice (CaMKIV null mice, 62.8 ± 4.3 % of baseline, $n = 4$; SA4503-treated CaMKIV null mice, 82.0 ± 3.8 % of baseline, $n = 4$). The elevation of CaMKII α (Thr-286) autophosphorylation by SA4503 was significantly inhibited by APV treatment at $50 \mu\text{M}$ (69.7 ± 3.1 % of control, $n = 4$) but not by nifedipine treatment at $10 \mu\text{M}$ (Fig. 5d, e).

CaMKIV Colocalizes with PSA-NCAM and Calbindin but not with a Glial Marker in the DG

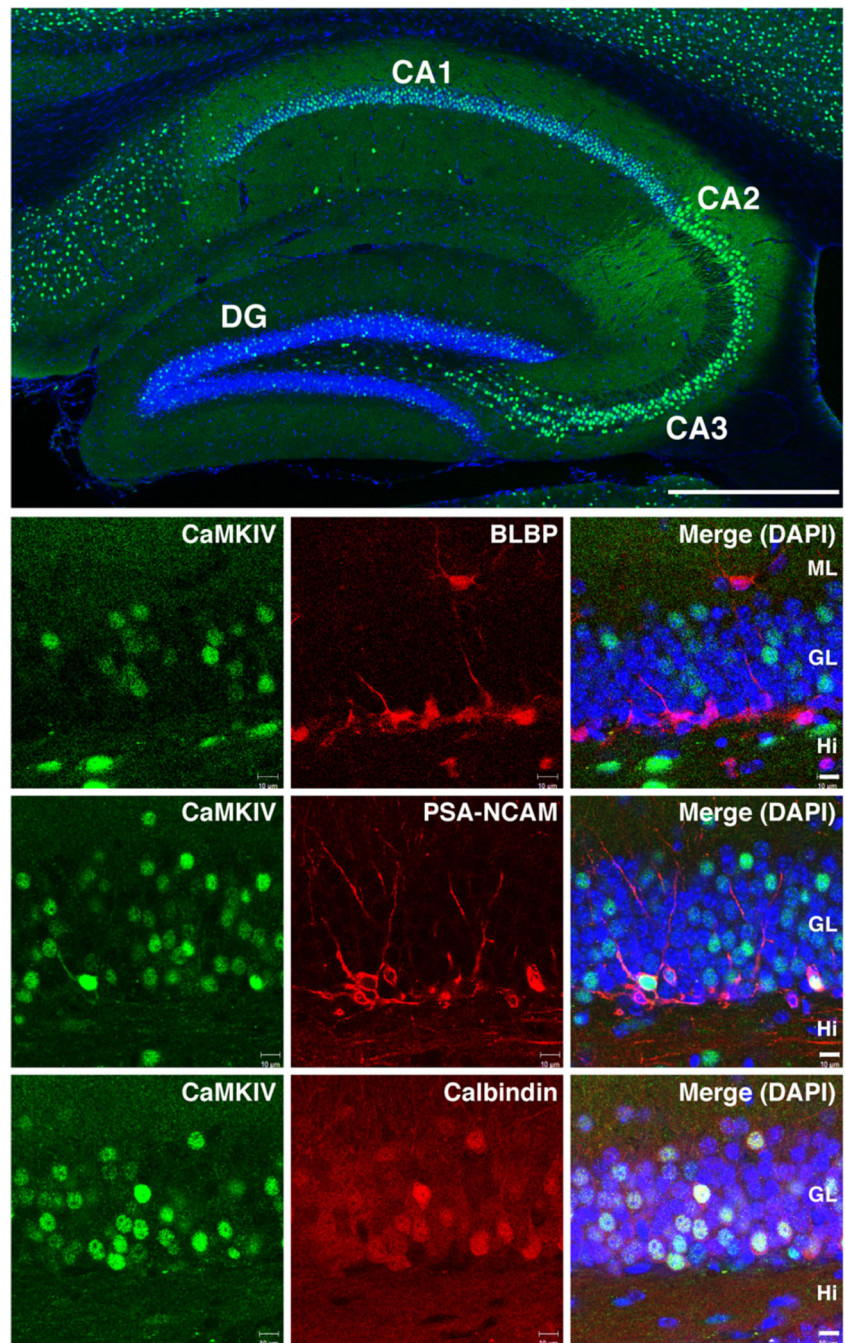
Finally, we assessed whether CaMKIV is expressed in immature neurons in addition to mature granule cells in the DG. To do so, we double-stained hippocampal slices with antibodies to CaMKIV and anti-BLBP (a marker of radial glia and astrocytes), anti-PSA-NCAM (a marker of newly generated immature granule cells), and anti-calbindin (a marker of mature granule cells) [37, 42, 43]. CaMKIV was expressed in both mature and immature granule cells in the DG not in either neural stem cells or astrocytes in the DG (Fig. 6).

Discussion

Phenotypes of Sig-1R null mice are associated with cognitive deficits, and anxiety- and depressive-like behaviors [6]. Since impaired adult hippocampal neurogenesis in DG correlates with depressive-like behaviors in OBX mice [7, 8] and Sig-1R null mice showed impaired adult hippocampal neurogenesis in DG [44], we hypothesized that depressive-like behaviors in CaMKIV null mice are associated with lost or impaired Sig-1R function in hippocampal DG and that paroxetine-resistant depression may be improved by treatment with Sig-1R agonists.

Consistent with previous studies showing that fluoxetine and fluvoxamine enhance adult hippocampal neurogenesis in the rodent DG [2, 4], we observed that fluvoxamine treatment ameliorated decreased neurogenesis seen in CaMKIV null mice. Surprisingly, the potent SSRI paroxetine failed to stimulate neurogenesis with concomitant lack of anti-depressive effects. The order of inhibitory constants (K_i) for inhibition of serotonin uptake into rat brain is: paroxetine ($K_i = 0.7 \text{ nM}$) >

Fig. 6 CaMKIV colocalizes with PSA-NCAM and calbindin but not with the glial marker BLBP in the DG. Confocal microscopy images showing double immunofluorescence staining of the adult DG for CaMKIV (green) and BLBP, PSA-NCAM, or calbindin (red). Merged images show nuclear staining with 4', 6-diamidino-2-phenylindole dihydrochloride (DAPI) (blue). Scale bars, 500 μ m in low magnification and 10 μ m in high magnification images



citalopram ($K_i=2.6$ nM)>sertraline ($K_i=3.4$ nM)>fluvoxamine ($K_i=6.2$ nM)>fluoxetine ($K_i=14$ nM) [45]. On the other hand, the order of affinity of SSRIs for the sigma-1 receptor is: fluvoxamine ($K_i=36$ nM)>sertraline ($K_i=57$ nM)>fluoxetine ($K_i=120$ nM)>citalopram ($K_i=292$ nM)>paroxetine ($K_i=1893$ nM) [46]. Thus, the lack of an anti-depressive effect by paroxetine in CaMKIV null mice suggests that Sig-1R stimulatory action rather than serotonin reuptake inhibition accounts for fluvoxamine's anti-depressive action. However, lack of amelioration by fluoxetine as reported by Sha et al.

[44] cannot be explained due to a low affinity for Sig-1R. Our hypothesis that fluvoxamine-induced anti-depressive action in CaMKIV null mice is mediated by Sig-1R stimulation was confirmed by the observation that the Sig-1R-specific agonist SA4503 ameliorates impaired adult hippocampal neurogenesis in DG and depressive behaviors in CaMKIV null mice.

Enhanced adult hippocampal neurogenesis is associated with activation of both the PI3K/Akt [8, 47, 48] and CREB/BDNF pathways [8, 47]. Activation of both pathways

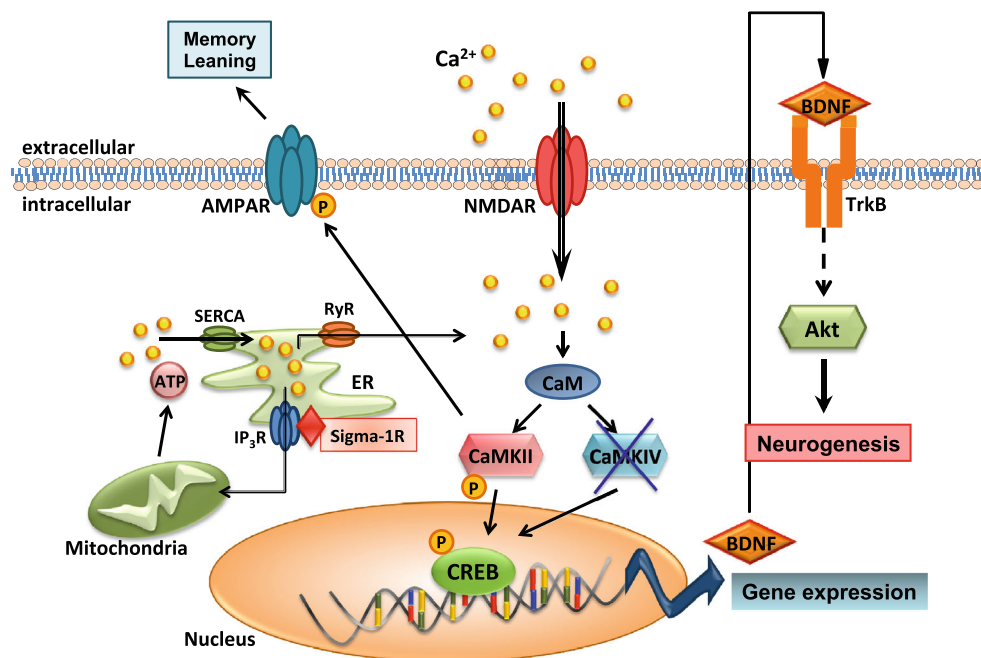
in neuronal progenitors plays an essential role in cell proliferation and maturation [38]. In the present study, stimulation of Sig-1R by fluvoxamine or SA4503 markedly activated both PI3K/Akt and CREB/BDNF signaling in DG of CaMKIV null mice. Although Akt and CaMKII phosphorylation was closely associated with CREB (Ser-133) phosphorylation, CaMKII likely accounts for the CREB phosphorylation and BDNF expression. This idea is also confirmed by the observation that expression of BDNF mRNA containing exons I or IV in the DG of CaMKIV null mice is upregulated by Sig-1R stimulation. Indeed, Sun et al. [49] reported that unlike CaMKIV, CaMKII regulates CREB activity through additional phosphorylation of CREB at Ser-142 residue (in addition to Ser-133). We also confirmed that CaMKII overexpression increases levels of BDNF transcripts containing exon IV in NG108-15 cells [50]. However, mechanisms underlying CaMKII activation by Sig-1R stimulation remain unclear. Stimulation of Sig-1R increases calcium transport from ER/SR to mitochondria, which in turn enhances ATP production [17]. Rescued ATP production may improve Ca^{2+} storage in ER by enhancing activity of the sarcoplasmic/endoplasmic Ca^{2+} -ATPase pump, which could promote Ca^{2+} -induced Ca^{2+} -release from the ER and in turn activate CaMKII activity in neurons.

Mechanisms underlying decreased neurogenesis seen in CaMKIV null mice are also largely unknown. As shown Fig. 6, CaMKIV is expressed ubiquitously in pyramidal neurons in both CA1 and CA3 regions and in DG granule cells. Interestingly, CaMKIV is expressed both in immature neurons stained with PSA-NCAM and in mature neurons positive for calbindin in the DG. Loss of CaMKIV in neural progenitors

may alter their proliferation. However, the total number of granule cells in the DG was comparable in wild-type and CaMKIV null mice. We previously documented that reduced CaMKII activity in CaMKII α heterozygous knockout mice increased the number of immature granule cells in the hippocampal DG but decreased the number of mature granule cells [51]. Moreover, the number of BrdU-positive cells slightly increased CaMKII α heterozygous knockout mice [51]. Thus, CaMKIV but not CaMKII α likely functions in proliferation or maturation of granule cells in the mouse DG. However, further studies are required to define the mechanism underlying decrease in Akt activity and neurogenesis in CaMKIV null mice.

Interestingly, Sig-1R stimulation enhances *N*-methyl-D-aspartate receptor (NMDAR)-evoked intracellular calcium mobilization [18, 52, 53]. In fact, the elevation of CaMKII activity by SA4503 was eliminated by NMDAR antagonist. The regulation of NMDAR activity by Sig-1R was also reported in Sig-1R null mice in which adult hippocampal neurogenesis is impaired via downregulation of NMDAR subunit NR2B [44]. Martina et al. [54] reported that a Sig-1R agonist inhibits small-conductance calcium-activated potassium channel in the hippocampus and consequently increased Ca^{2+} mobilization by an NMDAR-dependent mechanism. We here confirmed that SA4503 activation of Sig-1R increases CaMKII activity through NMDAR stimulation, thereby ameliorating the impaired hippocampal LTP seen in the DG of CaMKIV null mice. Akt activation by fluvoxamine and SA4503 is likely mediated by tyrosine kinase signaling associated with NMDAR activation [55] or NMDAR-dependent BDNF expression through CaMKII signaling

Fig. 7 Schematic representation of altered adult hippocampal neurogenesis in the DG. Stimulation of Sig-1R increases intracellular calcium mobilization through NMDARs in the plasma membrane or through the ER/SR via mitochondrial ATP production. Increased intracellular calcium increases CaMKII autophosphorylation and promotes CREB (Ser-133) phosphorylation and BDNF expression, which in turn increases Akt phosphorylation and promotes adult hippocampal neurogenesis



[56]. In addition, an essential role of link between Akt and CREB activities has been demonstrated in neural progenitor cells stimulated by fibroblast growth factor-2 (FGF-2), a factor that is essential for proliferation of hippocampal progenitors [57]. FGF-2 and insulin-like growth factor-1 (IGF-1) also reportedly enhance proliferation of adult hippocampal neural progenitors [57]. Both mitogens are known to stimulate Akt signaling [57]. In addition, conditional knockout of CREB in mice impairs in vivo proliferation of hippocampal neural progenitor cells [58]. Although cells that express FGF-2 and IGF-1 have not been precisely defined in the hippocampus, it is likely that both mitogens are derived from astrocytes based on studies of Shetty et al. [59]. In this context, our observation of immunohistochemical localization of Sig-1R in the hippocampus is particularly relevant. Sig-1R is expressed both in astrocytes and in both post- and presynaptic regions of neurons in DG. Thus, in CaMKIV null mice, Sig-1R stimulation may enhance adult hippocampal neurogenesis via Akt and/or BDNF pathways and synaptic efficacy through CaMKII activation in the DG. CaMKIV is not expressed in astrocytes and colocalizes with PSA-NCAM and calbindin but not with BLBP in the DG. We confirmed that CaMKIV is expressed in differentiating and mature dentate granule cells but not in neural stem cells or glial cells. However, it is also possible that Sig-1R stimulation of astrocytes accounts for Sig-1R stimulation-induced neurogenesis, as Cao et al. [60] used IP₃ receptor type 2 transgenic mice to show that ATP release from astrocytes is critical for effects of anti-depressants.

In conclusion, this study demonstrated that Sig-1R stimulation increases intracellular calcium mobilization and CaMKII/Akt signaling, possibly in a NMDAR-dependent or mitochondrial ATP production-dependent manner. Enhanced NMDAR and Akt signaling likely promote BDNF transcription, which would increase Akt phosphorylation via TrkB (Fig. 7). CaMKII and Akt signaling possibly ameliorate depressive-like behaviors through enhanced neurogenesis in CaMKIV null mice.

Acknowledgments This work was supported in part by grants from the Ministry of Education, Culture, Sports, Science and Technology, and the Ministry of Health and Welfare of Japan (22390109 to K.F.; 20790398 to S.M.), the Smoking Research Foundation (to K.F.), the Takeda Science Foundation (to S.M.), the Suzuken Memorial Foundation (to S.M.), the Yokoyama Foundation for Clinical Pharmacology (to S.M.) and the Comprehensive Brain Science Network (CBSN).

Authors Contributions S.M., H.S., Y.S., N.I., and Y.Y. performed the experiments. H.S. provided knockout mice. C.Z. and F.H. provided materials. S.M. and K.F. wrote the manuscript and designed the study.

Conflicts of Interest The authors declare no competing financial interests.

References

- Gould E, Tanapat P, Rydel T et al (2000) Regulation of hippocampal neurogenesis in adulthood. *Biol Psychiatry* 48:715–720
- Santarelli L, Saxe M, Gross C et al (2003) Requirement of hippocampal neurogenesis for the behavioral effects of antidepressants. *Science* 301(805):809
- Boldrini M, Underwood MD, Hen R et al (2009) Antidepressants increase neural progenitor cells in the human hippocampus. *Neuropsychopharmacology* 34:2376–2389
- Malberg JE, Duman RS (2003) Cell proliferation in adult hippocampus is decreased by inescapable stress: reversal by fluoxetine treatment. *Neuropsychopharmacology* 28(1562):1571
- Cobos EJ, Entrena JM, Nieto FR et al (2008) Pharmacology and therapeutic potential of sigma₁ receptor ligands. *Curr Neuropharmacol* 6:344–366
- Chevallier N, Keller E, Maurice T (2011) Behavioral phenotyping of knockout mice for the sigma-1 (σ 1) chaperone protein revealed gender-related anxiety, depressive-like and memory alterations. *J Psychopharmacol* 25:960–975
- Moriguchi S, Yamamoto Y, Ikuno T et al (2011) Sigma-1 receptor stimulation by dehydroepiandrosterone ameliorates cognitive impairment through activation of CaM kinase II, protein kinase C and extracellular signal-regulated kinase in olfactory bulbectomized mice. *J Neurochem* 117:879–891
- Moriguchi S, Shinoda Y, Yamamoto Y et al (2013) Stimulation of sigma-1 receptor by DHEA enhances synaptic efficacy and neurogenesis in the hippocampal dentate gyrus of olfactory bulbectomized mice. *PLoS ONE* 8:e60863
- Hanner M, Moebius FF, Flandorfer A et al (1996) Purification, molecular cloning, and expression of the mammalian σ 1 binding site. *Proc Natl Acad Sci U S A* 93:8072–8077
- Kekuda R, Prasad PD, Fei YJ et al (1996) Cloning and functional expression of the human type1 sigma receptor (hSigmaR1). *Biochem Biophys Res Commun* 229:553–558
- Seth P, Leibach FH, Ganapathy V (1997) Cloning and structural analysis of the cDNA and the gene encoding the murine type 1 sigma receptor. *Biochem Biophys Res Commun* 241:535–540
- Seth P, Fei YJ, Li HW et al (1998) Cloning and functional characterization of a sigma receptor from rat brain. *J Neurochem* 70:922–931
- Pan YX, Mey J, Xu J et al (1998) Cloning and characterization of a mouse σ ₁ receptor. *J Neurochem* 70:2279–2285
- Hayashi T, Su TP (2004) Sigma-1 receptors at galactosylceramide-enriched lipid microdomains regulate oligodendrocyte differentiation. *Proc Natl Acad Sci U S A* 101:14949–14954
- Palacios G, Muro A, Vela JM et al (2003) Immunohistochemical localization of the sigma1-receptor in oligodendrocytes in the rat central nervous system. *Brain Res* 961:92–99
- Hayashi T, Maurice T, Su TP (2000) Ca²⁺ signaling via sigma1-receptors: novel regulatory mechanism affecting intracellular Ca²⁺ concentration. *J Pharmacol Exp Ther* 293:788–798
- Shioda N, Ishikawa K, Tagashira H et al (2012) Expression of a truncated form of the endoplasmic reticulum chaperone protein, σ 1 receptor, promotes mitochondrial energy depletion and apoptosis. *J Biol Chem* 287:23318–23331
- Monnet FP, Mahe V, Robel P et al (1995) Neurosteroids, via sigma receptors, modulate the [³H] norepinephrine release evoked by *N*-methyl-D-aspartate in the rat hippocampus. *Proc Natl Acad Sci U S A* 92:3774–3778
- Gonzalez-Alvear GM, Werling LL (1994) Regulation of [³H] dopamine release from rat striatal slices by sigma receptor ligands. *J Pharmacol Exp Ther* 271:212–219
- Bito H, Deisseroth K, Tsien RW (1996) CREB phosphorylation and dephosphorylation: a Ca²⁺ and stimulus duration-dependent switch for hippocampal gene expression. *Cell* 87:1203–1214

21. Shaywitz AL, Greenberg ME (1999) CREB: a stimulus-induced transcription factor activated by a diverse array of extracellular signals. *Annu Rev Biochem* 68:821–861
22. West AE, Griffith EC, Greenberg ME (2002) Regulation of transcription factors by neuronal activity. *Nat Rev Neurosci* 3:921–931
23. Bourchouladze R, Fenguell B, Blendy J et al (1994) Deficient long-term memory in mice with a targeted mutation of the cAMP-responsive element-binding protein. *Cell* 79:59–68
24. Josselyn SA, Shi C, Carlezon WAJ et al (2001) Long-term memory is facilitated by cAMP response element-binding protein overexpression in the amygdala. *J Neurosci* 21:2404–2412
25. Impey S, Smith DM, Obrietan K et al (1998) Stimulation of cAMP response element (CRE)-mediated transcription during contextual learning. *Nat Neurosci* 1:595–601
26. Valverde O, Mantamadiotis T, Torrecilla M et al (2004) Modulation of anxiety-like behavior and morphine dependence in CREB-deficient mice. *Neuropsychopharmacology* 29:1122–1133
27. Maldonado R, Smadja C, Mazzucchelli M et al (1999) Altered emotional and locomotor responses in mice deficient in the transcription factor CREM. *Proc Natl Acad Sci U S A* 96:14094–14099
28. Barrot M, Olivier JD, Perrotti LI et al (2002) CREB activity in the nucleus accumbens shell controls gating of behavioral responses to stimuli. *Proc Natl Acad Sci U S A* 99:11435–11440
29. Ohmstede CA, Bland MM, Merrill BM et al (1991) Relationship of genes encoding Ca²⁺/calmodulin-dependent protein kinase α and calpermin: a gene within a page. *Proc Natl Acad Sci U S A* 88:5784–5788
30. Takao K, Tanda K, Nakamura K et al (2010) Comprehensive behavioral analysis of calcium/calmodulin-dependent protein kinase IV knockout mice. *PLoS ONE* 5:e9460
31. Shum FW, Ko SW, Lee YS et al (2005) Genetic alteration of anxiety and stress-like behavior in mice lacking CaMKIV. *Mol Pain* 1:22
32. Lee KH, Chatila TA, Ram RA et al (2009) Impaired memory of eyeblink conditioning in CaMKIV KO mice. *Behav Neurosci* 123:438–442
33. Song N, Nakagawa S, Izumi T et al (2012) Involvement of CaMKIV in neurogenic effect with chronic fluoxetine treatment. *Int J Neuropsychopharmacol* 16:803–812
34. Moriguchi S, Shioda N, Han F et al (2008) CaM kinase II and protein kinase C activations mediate enhancement of long-term potentiation by nefiracetam in the rat hippocampal CA1 region. *J Neurochem* 106:1092–1103
35. Fukunaga K, Horikawa K, Shibata S et al (2002) Ca²⁺/calmodulin-dependent protein kinase II-dependent long-term potentiation in the rat suprachiasmatic nucleus and its inhibition by melatonin. *J Neurosci Res* 70:799–807
36. Fukunaga K, Muller D, Miyamoto E (1995) Increased phosphorylation of Ca²⁺/calmodulin-dependent protein kinase II and its endogenous substrates in the induction of long term potentiation. *J Biol Chem* 270:6119–6124
37. Seki T, Arai Y (1993) Highly polysialylated neural cell adhesion molecule (NCAM-H) is expressed by newly generated granule cells in the dentate gyrus of the adult rat. *J Neurosci* 13:2351–2358
38. Li BS, Ma W, Zhang L et al (2001) Activation of phosphatidylinositol-3 kinase (PI-3 K) and extracellular regulated kinases (Erk1/2) is involved in muscarinic receptor-mediated DNA synthesis in neural progenitor cells. *J Neurosci* 21:1569–1579
39. Zheng F, Zhou X, Luo Y et al (2011) Regulation of brain-derived neurotrophic factor exon IV transcription through calcium responsive elements in cortical neurons. *PLoS ONE* 6:e28441
40. Kidane AH, Heinrich G, Dirks RPH et al (2009) Differential neuroendocrine expression of multiple brain-derived neurotrophic factor transcripts. *Endocrinology* 150:1361–1368
41. Ruscher K, Shamloo M, Rickhag M et al (2011) The sigma-1 receptor enhances brain plasticity and functional recovery after experimental stroke. *Brain* 134:732–746
42. Feng L, Hatten ME, Heintz N (1994) Brain lipid-binding protein (BLBP): a novel signaling system in the developing mammalian CNS. *Neuron* 12:895–908
43. Jia C, Halpern M (2003) Calbindin D28K immunoreactive neurons in vomeronasal organ and their projections to the accessory olfactory bulb in the rat. *Brain Res* 977:261–269
44. Sha S, Qu WJ, Li L et al (2013) Sigma-1 receptor knockout impairs neurogenesis in dentate gyrus of adult hippocampus via down-regulation of NMDA receptors. *CNS Neurosci Ther* 19:705–713
45. Hiemke C, Hrtter S (2000) Pharmacokinetics of selective serotonin reuptake inhibitors. *Pharmacol Ther* 85:11–28
46. Narita N, Hashimoto K, Tomitaka S et al (1996) Interactions of selective serotonin reuptake inhibitors with subtypes of sigma receptors in rat brain. *Eur J Pharmacol* 307:117–119
47. Wu H, Lu D, Jiang H et al (2008) Simvastatin-mediated upregulation of VEGF and BDNF, activation of the PI3K/Akt pathway, and increase of neurogenesis are associated with therapeutic improvement after traumatic brain injury. *J Neurotrauma* 25:130–139
48. Shioda N, Han F, Morioka M et al (2008) Bis(1-oxy-2-pyridinethiolato)oxovanadium(IV) enhances neurogenesis via phosphatidylinositol 3-kinase/Akt and extracellular signal regulated kinase activation in the hippocampal subgranular zone after mouse focal cerebral ischemia. *Neuroscience* 155:876–887
49. Sun P, Enslin H, Myung PS et al (1994) Differential activation of CREB by Ca²⁺/calmodulin-dependent protein kinases type II and type IV involves phosphorylation of a site that negatively regulates activity. *Genes Dev* 8:2527–2539
50. Takeuchi Y, Fukunaga K, Miyamoto E (2002) Activation of nuclear Ca²⁺/calmodulin-dependent protein kinase II and brain-derived neurotrophic factor gene expression by stimulation of dopamine D2 receptor in transfected NG108-15 cells
51. Yamasaki N, Maekawa M, Kobayashi K et al (2008) Alpha-CaMKII deficiency causes immature dentate gyrus, a novel candidate endophenotype of psychiatric disorders. *Mol Brain* 1:6
52. Irwin RP, Lin SZ, Rogawski MA et al (1994) Steroid potentiation and inhibition of N-methyl-D-aspartate receptor-mediated intracellular Ca²⁺ response: structure-activity studies. *J Pharmacol Exp Ther* 271:677–682
53. Chen L, Miyamoto Y, Furuya K et al (2007) PREGS induces LTP in the hippocampal dentate gyrus of adult rats via the tyrosine phosphorylation of NR2B coupled to ERK/CREB signaling. *J Neurophysiol* 98:1538–1548
54. Martina M, Turcotte ME, Halman S et al (2007) The sigma-1 receptor modulates NMDA receptor synaptic transmission and plasticity via SK channels in rat hippocampus. *J Physiol* 578:143–157
55. Crossthwaite AJ, Valli H, Williams RJ (2004) Inhibiting Src family tyrosine kinase activity blocks glutamate signaling to ERK1/2 and Akt/PKB but not JNK in cultured striatal neurons. *J Neurochem* 88:1127–1139
56. Du J, Feng L, Yang F et al (2000) Activity- and Ca²⁺-dependent modulation of surface expression of brain-derived neurotrophic factor receptors in hippocampal neurons. *J Cell Biol* 150:1423–1434
57. Peltier J, O'Neill A, Schaffer DV (2007) PI3K/Akt and CREB regulate adult neural hippocampal progenitor proliferation and differentiation. *Dev Neurobiol* 67:1348–1361
58. Mantamadiotis T, Lemberger T, Bleckmann SC et al (2002) Disruption of CREB function in brain leads to neurodegeneration. *Nat Genet* 31:47–54
59. Shetty AK, Hattiangady B, Shetty GA (2005) Stem/progenitor cell proliferation factors FGF-2, IGF-1, and VEGF exhibit early decline during the course of aging in the hippocampus: role of astrocytes. *Glia* 51:173–186
60. Cao X, Li LP, Wang Q et al (2013) Astrocyte-derived ATP modulates depressive-like behaviors. *Nat Med* 19:773–777